Published in final edited form as:
ASAIO J. 2013 ; 59(3): 275–283. doi:10.1097/MAT.0b013e31828e4d80.

Towards Optimization of a Novel Trileaflet Polymeric Prosthetic Heart Valve Via Device Thrombogenicity Emulation (DTE)

Thomas E. Claiborne[*], **Michalis Xenos**[†], **Jawaad Sheriff**[*], **Wei-Che Chiu**[*], **Joao Soares**[*], **Yared Alemu**[*], **Shikha Gupta**[*], **Stefan Judex**[*], **Marvin J. Slepian**[*,‡], and **Danny Bluestein**[*]

[*]Dept. of Biomedical Engineering, Stony Brook University, Stony Brook, NY

[†]Dept. of Mathematics, University of Ioannina, Greece

[‡]Department of Medicine and Biomedical Engineering, Sarver Heart Center, University of Arizona, Tucson, AZ

Abstract

Aortic stenosis the is most prevalent and life threatening form of valvular heart disease. It is primarily treated via open-heart surgical valve replacement with either a tissue or mechanical prosthetic heart valve (PHV), each prone to degradation and thrombosis, respectively. Polymeric PHVs may be optimized to eliminate these complications, and they may be more suitable for the new transcatheter aortic valve replacement (TAVR) procedure and in devices like the Total Artificial Heart. However, the development of polymer PHVs has been hampered by persistent *in vivo* calcification, degradation, and thrombosis. To address these issues, we have developed a novel surgically implantable polymer PHV comprised of a new thermoset polyolefin called xSIBS, in which key parameters were optimized for superior functionality via our Device Thrombogenicity Emulation (DTE) methodology. In this parametric study, we compared our homogeneous optimized polymer PHV to a prior composite polymer PHV and to a benchmark tissue valve. Our results show significantly improved hemodynamics and reduced thrombogenicity in the optimized polymer PHV compared to the other valves. These results indicate that our new design may not require anticoagulants and may be more durable than its predecessor, and validates the improvement, towards optimization, of this novel polymeric PHV design.

Keywords

platelet activation; transcatheter; artificial heart; numerical analysis; aortic stenosis

Corresponding Author: Prof. Danny Bluestein, Ph.D., Stony Brook University HSC T18 RM 030, Stony Brook, NY 11794, Tel: (631) 444-2156, Fax: (631) 444-6646, danny.bluestein@sunysb.edu.

Disclaimers: none

Disclosures: Dr. Slepian is Founder and Chief Scientific Officer of SynCardia Systems, Inc. Innovia LLC and SynCardia are partners in the NIH-NIBIB funded Quantum project. This study is supported by the NIH-NIBIB (Quantum Award Phase I R01, EB008004-01, DB, and Quantum Award: Implementation Phase II-1U01EB012487-0, DB). The authors wish to thank Dr. Gaurav Girdhar for contributions to the development of the HSD and DTE methods.

CONFLICT OF INTEREST STATEMENT Dr. Slepian is Founder and CSO of SynCardia Systems, Inc. Innovia LLC and SynCardia are partners in the NIH-NIBIB funded Quantum project.

INTRODUCTION

Aortic stenosis (AS) afflicts approximately 0.9% of the Unites States population with 2.8% of patients above 75 having moderate to severe AS.[1] Commercially available tissue and mechanical PHVs for aortic valve replacement are prone to degradation and thrombosis, respectively.[2] Up to 33% of patients requiring valve replacement are deemed inoperable due to significant co-morbidities.[3] The new transcatheter aortic valve replacement (TAVR) procedure currently serves this previously unmet clinical need.[4] However, current TAVR devices use tissue valves, which may sustain collagen fiber damage during deployment.[5,6] In an attempt to address these limitations, we have developed a novel trileaflet polymeric PHV. The valve prototype presented here has been designed for surgical implantation, but the design lends itself to TAVR.

Relatively few numerical studies were performed in trileaflet valves, particularly with respect to predicting platelet activation and durability. The recent interest in TAVR and increasing use of pulsatile mechanical circulatory support devices currently employing mechanical PHVs (e.g., the Total Artificial Heart[7] and the Penn State Pediatric Ventricular Assist Device[8]) have recently motivated new numerical studies of trileaflet valves.[9-13]

Development of polymer PHVs has been hampered by persistent *in vivo* calcification, degradation, and thrombosis.[14] Therefore, we have focused on optimizing thromboresistance and durability of our current prototype. We use a new proprietary thermoset polyolefin, xSIBS,[15] which has been designed to increase the strength and durability of the thermoplastic SIBS elastomer[16,17] while retaining its super-biostability. To show equivalence to currently approved PHVs in terms of hemodynamics and thrombogenicity[14] we have applied our DTE methodology,[18-20] comparing three valves: (1) the original SIBS-Dacron composite PHV[21,22] (Innovia LLC, Miami, FL) (Fig. 1A), (2) a commercially available tissue 'gold standard' PHV with fine clinical performance,[23] the Carpentier-Edwards Perimount Magna Bioprosthetic valve (Edwards Lifesciences, Irvine, CA) (Fig. 1 B&C), and (3) our new DTE-optimized homogeneous xSIBS-PHV (Fig. 1D). Briefly, the DTE methodology is a combination of numerical and experimental techniques for optimizing the thromboresistance of blood contacting devices.[18-20] In this hemodynamically optimized design we have altered key geometric parameters to produce a clinically viable polymeric PHV.

METHODS

Three trileaflet valves, each with nominal entrance internal diameters of 19 mm, equivalent to a tissue annulus diameter of 21 mm, were compared using our DTE methodology.[18-20] The 3-D geometry of the tissue valve was obtained using micro-CT (μCT40, Scanco Medical, SUI). Scans were conducted at 36 μm isotropic resolution with an energy level of 70kV and 114μA (Fig. 1 C). The 3-D geometry was reconstructed using Mimics (Materialise, Leuven, Belgium) and imported into Gambit (ANSYS, Inc. Canonsburg, PA), where a mesh was generated for finite element analysis (FEA).

The novel PHV geometry was designed using SolidWorks (DS SolidWorks Corp., Waltham, MA). The radial cross-sectional profile of the leaflets was modified from uniform to variable thickness with regions of computed higher or lower stresses thickened or thinned, respectively. The shape of the leaflet was changed from cylindrical to hemispherical (Fig. 2) and coaptation surface maximized by designing a flat leaflet profile (Fig. 2). The valve's stent was altered by smoothing surfaces and edges and widening the exit orifice by 2 mm (Fig. 2).

FEA

Mechanical Properties of xSIBS for Numerical Analysis—Uniaxial tensile tests to failure were performed on samples of xSIBS for computing the numerical material model constants. The xSIBS was compression molded (Grobet USA Hot Press Carlstadt, NJ) with simultaneous heating (240°C for 30 min.) to induce cross-linking via a Diels-Alder reaction. Tensile tests were performed according to ASTM D882-12/D638-10 (n=5) with a pull rate 5 mm/min to break (Instron 3343 with 1000 N force transducer and Bluehill software, Norwood, MA), and stress vs. strain curves were generated.

Validation of the Numerical Material Model—Tensile tests were simulated via structural FEA using ADINA (ADINA R&D, Inc. Watertown, MA). Data from xSIBS tensile tests were used as the input for the isotropic hyperelastic Mooney-Rivlin material model given by the strain energy function (1):[24]

$$W_D = C_1 (I_1 - 3) + C_2 (I_2 - 3) + D (exp (D_2 (I_1 - 3)) - 1) \quad (1)$$

Constants C_1 and C_2 were computed for best fit to the experimental data.

Structural FEA—A simulated normal diastolic pressure load (80 mmHg) was applied to the aortic surface of the valves' leaflets via structural FEA. The geometry was discretized with unstructured 4-node tetrahedral elements. Mesh independence studies were conducted at three mesh densities (0.0008, 0.0004, 0.00025 times length scale, corresponding to approx. 12,500, 55,000, and 170,000 elements), establishing the mesh density at 0.0005 (approx. 25,000-30,000 elements, based on the specific valve). Contact conditions were applied to the ventricular surface of the leaflets to model the valve closure.[25] Each valve's corresponding material properties were: (1) xSIBS tensile test data for the optimized valve, (2) tensile test data for the original composite SIBS-Dacron PHV,[22] and (3) fixed pericardial patch Moony-Rivlin constants C_1, C_2, D_1, D_2 from Tang *et al.*[26] for the tissue valve. The FEA smoothened effective stress maps were qualitatively compared. Additionally, structural FEA studies were performed using full cardiac cycle transvalvular pressure gradient loading[22] applied to the aortic and ventricular surfaces of the leaflets to obtain the open and closed valve geometries for a subsequent two-phase computational fluid dynamics (CFD) studies.

CFD

Two-phase CFD studies were conducted in 6 valve geometries (3 open and 3 closed) embedded in a rigid straight tube using Fluent (ANSYS, Inc. Canonsburg, PA)[18] employing a turbulent flow model (Wilcox k-ω) for the open valve, and assuming laminar flow for the closed valve. Blood was modeled as a Newtonian fluid with a dynamic viscosity of 3.5 cP and a density of 1050 kg/m^3. In forward flow simulations, a decelerating systolic velocity profile[27] was imposed at the inlet and zero pressure at the outlet. In regurgitant flow simulations, a constant velocity of 0.05 m/s was applied at the inlet and zero pressure at the outlet. In each study, 350 ms of flow were simulated, with approx. 30,000 neutrally buoyant spherical platelet analogs (3 μm diameter) seeded into the flow, and their stress accumulation (SA) was computed using a linear model.[18]

Platelet Trajectory Selection for Hemodynamic Shearing Device (HSD) Experiments—In CFD post processing, spherical regions of interest (ROI), r = 1 mm, were queried at the three commissures near the wall and at the core flow, all near the leaflets' free edges. These ROIs or 'hot spots' contain shear stress levels that may activate the platelets.[27] A probability density function (PDF) was computed for each ROI (4 per valve, total 24), and a single platelet trajectory representing the most frequently occurring

SA was selected for each ROI. The stress-time waveforms from these trajectories were programmed into our Hemodynamic Shearing Device (HSD) for *in vitro* human platelet activation studies.[18,19]

Platelet Activation Measurements—Blood was obtained from healthy volunteers of both sexes screened for antiplatelet medication and a history of smoking following institutional IRB protocols. Platelet rich plasma was separated from whole blood via centrifuge and sepharose gel filtered in a Hepes modified Tyrode's platelet buffer to obtain freshly isolated platelets. Viscosity of the platelet buffer was adjusted to 7.0 and 8.0 cP corresponding to max. waveform shear stresses of 700 and 800 dynes/cm^2 using Dextran (MW 150,000 Sigma-Aldrich). Our platelet activation state (PAS) assay was used to measure thrombin generation rates.[28] Each set of 12 experiments for both forward and regurgitant flow were performed using platelets from the same donor within 6 hours of obtaining gel filtered platelets (n=8 sets: 4 open & 4 closed, total 96 experiments).

Statistical Analysis

Numerical: The SA from the platelet trajectories was collapsed into a PDF, called the 'Thrombogenic Footprint' of each valve (Fig. 6).[18,19] Results were compared via one-way ANOVA with significance level α=0.05. Bootstrapping was used to equalize population sizes.[18]

Experimental: The change in (Δ) PAS was calculated over the 10 min HSD experiment. The mean ΔPAS for 4 sets was plotted for each of the four ROIs (commissures 1-3 and the core) with standard error bars for both forward and regurgitant flow. One-way ANOVA was used with significance level α=0.05.

RESULTS

FEA

xSIBS Mechanical Properties—The xSIBS samples exhibited nonlinear hyperelastic responses by enduring >100% strain will full elastic recovery and exhibiting strain stiffening beyond 100% strain (Fig. 3A). The mean ultimate strength was approximately 5,000 kPa.

Validation of the Numerical Material Model—The simulated tensile tests produced stress-strain curves that matched the experimental data in strains <20% (Figs. 3 B&C); a sufficient range for characterizing the stress-strain response in the valve leaflets.

Structural Stress Analysis

The optimized design demonstrated significantly reduced stress concentrations at the commissures, across the leaflet belly, and on the leaflet free edge as compared to the original composite polymer and tissue PHVs (Fig. 4).

CFD

Significant flow characteristics of the three valves are presented in Table 1.

Open Valves-Forward Flow

Particle Dispersion—The particle bolus through the open valves exhibited a triangular shaped structure (Fig. 5 top row), with unique patterns in each valve: the optimized polymer PHV exhibited three diverging spherical boluses, the pattern was more triangular and organized in the tissue PHV, while the original composite PHV exhibited a less triangular

and more disorganized pattern. In all three valves, low velocity recirculation of platelets was observed on the aortic surface of the leaflets and near the wall, with the bulk of the platelets passing quickly through the domain.

Hot Spots: Comparison of the four selected platelet trajectories show the least disturbed pathlines occurring near the wall for the optimized PHV (Fig. 6, top), which also produced the lowest instantaneous stress and least dynamic platelet stress history waveforms compared to the tissue and original composite polymer PHVs (Fig. 9, bottom). An axial cross-sectional view of the velocity vectors shows that the tissue valve has a high velocity jet emanating downstream from the leaflets' free edges as compared to the original composite and optimized polymer PHVs (Fig. 6, bottom).

Thrombogenic Footprints: The PDFs of the open valves show that the dominant mode of the optimized PHV is shifted towards the lower SA range as compared to the composite polymer and tissue PHVs (Fig. 8, top), with significant differences between the designs ($p < 0.01$).

Closed Valves-Regurgitant Flow

Particle Dispersion: Particle dispersion patterns were dominated by four small jets emanating from the three commissures and the core (Fig. 5, bottom). In the optimized PHV, the four particle jets remain distinct as they move downstream, the commissure jets in the original composite PHV exhibit prominent recirculation zones near the ventricular surface of the leaflets, whereas in the tissue valve, the jets exhibited disorganized mixing downstream.

Hot Spots: Comparison of the four selected platelet trajectories in each valve showed the least disturbed (Fig. 7, top) and less dynamic stress loading (Fig. 10, bottom) in the optimized design as compared to the composite polymer and tissue PHVs. An axial cross-sectional view of the velocity vectors shows that the tissue PHV produced a wide medium velocity central jet, the original composite PHV produced small high velocity jets with prominent recirculation near the leaflets, and the optimized polymer PHV produced tightly organized jets skewed towards the wall with no apparent recirculation (Fig. 7, bottom).

Thrombogenic Footprints: The PDFs of the closed valves (Fig. 8, bottom) are bimodally distributed. The lower SA range first mode (leftmost) represents platelets trapped upstream of the closed valves, and the rightmost modes represent platelets that escaped through the valves. The second mode of the optimized polymer PHV is shifted furthest to the lower SA range with significant differences between the valves ($p < 0.01$).

Platelet Activation Measurements—The mean ΔPAS correlated with the calculated mean SA of each corresponding trajectory (Table 2). The commissure trajectories produced higher ΔPAS values, with the open valves producing higher ΔPAS values than the closed valves (Figs. 9 & 10, top). In both forward and regurgitant flow, the optimized valve commissure trajectories produced drastically lower ΔPAS compared to the composite polymer and tissue PHVs ($p<0.01$).

DISCUSSION

In this study we have compared three trileaflet valves: (1) non-optimized original composite SIBS-Dacron PHV (Innovia), (2) a 'gold-standard' Carpentier-Edwards Perimount Magna tissue valve (Edwards Lifesciences), and (3) a novel DTE-optimized homogeneous xSIBS-PHV. We have demonstrated that the optimized xSIBS-PHV produced: (1) the lowest pressure gradient in forward flow, lowest max. velocity in forward flow, and the highest

effective orifice area (2) the least disturbed flow in both forward and regurgitant flow, (3) the lowest platelet SA in both forward and regurgitant flow, and (4) the lowest ΔPAS in both forward and regurgitant flow. These results indicate a comparatively superior performance of the DTE-optimized valve, which may not require anticoagulants and be more durable than its predecessor.

Optimization was achieved by altering key geometric features of the new valve in addition to using a new material. The thermoset polyolefin, xSIBS,[15] an improvement over the thermoplastic elastomer SIBS,[16,17] has demonstrated tissue-like hyperelastic behavior and increased tensile strength. The original composite SIBS-Dacron PHV design featured a cast leaflet material of uniform thickness attached via polyester sutures to a high styrene content molded SIBS stent.[21,22] Our novel optimized PHV was designed to be compression molded entirely in one step using only xSIBS. This allows for the creation of precision shapes and facilitates the thermal cross linking of xSIBS. The leaflet thickness was altered at key locations to achieve optimal stress distributions for increased durability. Additionally, the valve stent geometry was modified to further improve its hemodynamics by widening the exit orifice diameter by 2 mm and smoothening the edges. The combination of these design modifications produced significantly better hemodynamics and reduced thrombogenicity of our new valve as compared to both the original composite polymer and tissue PHVs. The significantly lower stresses predicted by structural FEA indicates that the optimized PHV may have comparatively enhanced long-term durability. However, further prototype testing is required before definitive conclusions can be made.

The two-phase CFD simulations provided a detailed depiction of unique flow patterns created by each valve design. The results clearly indicate that the optimized PHV has an advantage in both the forward and regurgitant flow phases. The ‘thrombogenic footprints’ or PDFs show that in the optimized valve the dominant modes are shifted toward the (less thrombogenically risky) lower SA range as compared to the other two valves. We have previously measured bulk platelet activation in a pulsatile left ventricular assist device in both the original composite polymer and the tissue PHVs,[29] and found a significantly lower platelet activation rate in the former, which further supports our thrombogenic footprint comparisons.

Emulating in our HSD the statistically representative ‘hot spot’ platelet stress loading waveforms extracted from the computed platelet trajectories in CFD, and measuring the resultant platelet activity allows us, by proxy, to validate the predictions of the numerical simulations. The optimized PHV platelet trajectories produced significantly lower ΔPAS in all cases studied. The mean ΔPAS values correlated well with the predicted mean SA values from CFD across all selected trajectories, validating our numerical results. The optimized design significantly reduced the occurrence of ‘hot spot’ regions in the valve, indicating that our novel PHV design may not require anticoagulants.

Comparable numerical studies of trileaflet valve hemodynamics are scant. Sirois *et al.* have performed a two-phase CFD evaluation of a tissue valve in order to investigate hemolysis and platelet activation potential.[12] Dwyer *et al.* performed important yet comparatively simpler CFD simulations of an idealized open TAVR tissue valve.[9,10] Our studies proceed beyond this to compute multiple platelet trajectories and predict the thrombogenic potential of the valves. Lim *et al.* examined effects of leaflet coaptation curvature on stress distribution in pericardial valves using FEA and found lowest stresses in curved profile leaflets.[30] Our studies of leaflet curvature found lower stresses in the flat profile, attributed to its dramatically increased coaptation surface area. Other factors influencing the leaflet stress distribution include leaflet material, thickness, stent attachment design, and stent post stiffness.

Limitations to this study include simplifying assumptions in the numerical models, the inability to emulate all platelet trajectories in our HSD, the use of isolated platelets instead of whole blood, and the computation of platelet SA using a phenomenological linear model.

CONCLUSIONS

We have optimized a novel trileaflet polymeric prosthetic heart valve design using our DTE methodology. The optimized polymer PHV was compared to a prior composite polymer design and to a 'gold standard' tissue valve. Superior performance was observed with our optimized valve in terms of its projected structural durability and its hemodynamic and thrombogenic performance, indicating that the optimized valve design may be nonthrombogenic and more durable than its predecessor. We have verified the efficacy of our DTE methodology in trileaflet valves. This strategy has advanced polymeric valves closer to clinical viability.

Acknowledgments

This study is supported by the NIH-NIBIB (Quantum Award Phase I R01, EB008004-01, DB, and Quantum Award: Implementation Phase II-1U01EB012487-0, DB). The authors wish to thank Dr. Gaurav Girdhar for contributions to the development of the HSD and DTE methods.

REFERENCES

1. Go AS, Mozaffarian D, Roger VL, et al. Heart Disease and Stroke Statistics--2013 Update A Report From the American Heart Association. Circulation. Dec 12.2012
2. Rahimtoola SH. Choice of prosthetic heart valve in adults an update. J Am Coll Cardiol. Jun 1; 2010 55(22):2413–2426. [PubMed: 20510209]
3. Rosengart TK, Feldman T, Borger MA, et al. Percutaneous and minimally invasive valve procedures: a scientific statement from the American Heart Association Council on Cardiovascular Surgery and Anesthesia, Council on Clinical Cardiology, Functional Genomics and Translational Biology Interdisciplinary Working Group, and Quality of Care and Outcomes Research Interdisciplinary Working Group. Circulation. Apr 1; 2008 117(13):1750–1767. [PubMed: 18332270]
4. Makkar RR, Fontana GP, Jilaihawi H, et al. Transcatheter Aortic-Valve Replacement for Inoperable Severe Aortic Stenosis. N Engl J Med. Mar 26.2012
5. Zegdi R, Bruneval P, Blanchard D, Fabiani JN. Evidence of leaflet injury during percutaneous aortic valve deployment. Eur J Cardiothorac Surg. Jul; 2011 40(1):257–259. [PubMed: 21167732]
6. de Buhr W, Pfeifer S, Slotta-Huspenina J, Wintermantel E, Lutter G, Goetz WA. Impairment of pericardial leaflet structure from balloon-expanded valved stents. J Thorac Cardiovasc Surg. Jun; 2012 143(6):1417–1421. [PubMed: 22244562]
7. Platis A, Larson DF. CardioWest temporary total artificial heart. Perfusion. Sep; 2009 24(5):341–346. [PubMed: 19917572]
8. Roszelle BN, Deutsch S, Manning KB. A parametric study of valve orientation on the flow patterns of the Penn State pulsatile pediatric ventricular assist device. ASAIO J. Jul-Aug;2010 56(4):356–363. [PubMed: 20559131]
9. Dwyer HA, Matthews PB, Azadani A, Ge L, Guy TS, Tseng EE. Migration forces of transcatheter aortic valves in patients with noncalcific aortic insufficiency. J Thorac Cardiovasc Surg. Nov; 2009 138(5):1227–1233. [PubMed: 19748632]
10. Dwyer HA, Matthews PB, Azadani A, et al. Computational fluid dynamics simulation of transcatheter aortic valve degeneration. Interact Cardiovasc Thorac Surg. Aug; 2009 9(2):301–308. [PubMed: 19414489]
11. Sun W, Li K, Sirois E. Simulated elliptical bioprosthetic valve deformation: Implications for asymmetric transcatheter valve deployment. J Biomech. Sep 2.2010

12. Sirois E, Sun W. Computational evaluation of platelet activation induced by a bioprosthetic heart valve. Artif Organs. Feb; 2011 35(2):157–165. [PubMed: 21083829]
13. Wang Q, Sirois E, Sun W. Patient-specific modeling of biomechanical interaction in transcatheter aortic valve deployment. J Biomech. Jun 12.2012
14. Claiborne TE, Slepian MJ, Hossainy S, Bluestein D. Polymeric trileaflet prosthetic heart valves: evolution and path to clinical reality. Expert Rev Med Devices. Nov; 2012 9(6):577–594. [PubMed: 23249154]
15. Pinchuk L, Zhou Y. Inventor. Crosslinked Polyolefins For Biomedical Applicatios And Method of Making Same. 2009
16. Pinchuk L, Wilson GJ, Barry JJ, Schoephoerster RT, Parel JM, Kennedy JP. Medical applications of poly(styrene-block-isobutylene-block-styrene) ("SIBS"). Biomaterials. Feb; 2008 29(4):448–460. [PubMed: 17980425]
17. El, Fray M.; Prowans, P.; Puskas, JE.; Altstadt, V. Biocompatibility and fatigue properties of polystyrene-polyisobutylene-polystyrene, an emerging thermoplastic elastomeric biomaterial. Biomacromolecules. Mar; 2006 7(3):844–850. [PubMed: 16529422]
18. Xenos M, Girdhar G, Alemu Y, et al. Device Thrombogenicity Emulator (DTE)--design optimization methodology for cardiovascular devices: a study in two bileaflet MHV designs. J Biomech. Aug 26; 2010 43(12):2400–2409. [PubMed: 20483411]
19. Girdhar G, Xenos M, Alemu Y, et al. Device Thrombogenicity Emulation: A Novel Method for Optimizing Mechanical Circulatory Support Device Thromboresistance. PLoS One. 2012; 7(3):e32463. [PubMed: 22396768]
20. Bluestein D, Einav S, Slepian MJ. Device thrombogenicity emulation: A novel methodology for optimizing the thromboresistance of cardiovascular devices. J Biomech. Dec 6.2012
21. Gallocher SL, Aguirre AF, Kasyanov V, Pinchuk L, Schoephoerster RT. A novel polymer for potential use in a trileaflet heart valve. J Biomed Mater Res B Appl Biomater. Nov; 2006 79(2): 325–334. [PubMed: 16649171]
22. Gallocher, SL. Durability assessment of polymer trileaflet heart valves. Biomedical Engineering, Florida International University; Miami: 2007.
23. Borger MA, Nette AF, Maganti M, Feindel CM. Carpentier-Edwards Perimount Magna valve versus Medtronic Hancock II: a matched hemodynamic comparison. Ann Thorac Surg. Jun; 2007 83(6):2054–2058. [PubMed: 17532395]
24. Bathe, K-J. Nonlinear finite element analysis and ADINA : proceedings of the 6th ADINA Conference, Massachusetts Institute of Technology. Pergamon Press; New York: Jun 10-12. 1987 1987
25. Peter DA, Alemu Y, Xenos M, et al. Fluid structure interaction with contact surface methodology for evaluation of endovascular carotid implants for drug-resistant hypertension treatment. J Biomech Eng. Apr.2012 134(4):041001. [PubMed: 22667676]
26. Tang D, Yang C, Geva T, Gaudette G, Del Nido PJ. Multi-Physics MRI-Based Two-Layer Fluid-Structure Interaction Anisotropic Models of Human Right and Left Ventricles with Different Patch Materials: Cardiac Function Assessment and Mechanical Stress Analysis. Comput Struct. Jun; 2011 89(11-12):1059–1068. [PubMed: 21765559]
27. Bluestein D, Rambod E, Gharib M. Vortex shedding as a mechanism for free emboli formation in mechanical heart valves. J Biomech Eng. Apr; 2000 122(2):125–134. [PubMed: 10834152]
28. Jesty J, Bluestein D. Acetylated prothrombin as a substrate in the measurement of the procoagulant activity of platelets: elimination of the feedback activation of platelets by thrombin. Anal Biochem. Jul 15; 1999 272(1):64–70. [PubMed: 10405294]
29. Claiborne TE, Girdhar G, Gallocher-Lowe S, et al. Thrombogenic potential of Innovia polymer valves versus Carpentier-Edwards Perimount Magna aortic bioprosthetic valves. ASAIO J. Jan-Feb;2011 57(1):26–31. [PubMed: 20930618]
30. Lim KH, Candra J, Yeo JH, Duran CM. Flat or curved pericardial aortic valve cusps: a finite element study. J Heart Valve Dis. Sep; 2004 13(5):792–797. [PubMed: 15473482]
31. Hakki AH, Iskandrian AS, Bemis CE, et al. A simplified valve formula for the calculation of stenotic cardiac valve areas. Circulation. May; 1981 63(5):1050–1055. [PubMed: 7471364]

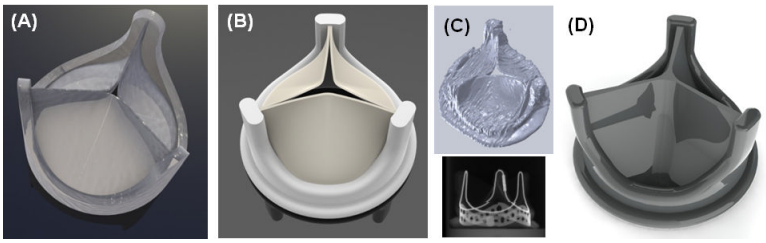

Figure 1.
CAD images of the valves: (A) original Innovia composite SIBS-Dacron polymer PHV, (B) Carpentier-Edwards Perimount Magna Bioprosthesis (Edwards Lifesciences), (C) microCT scan and reconstructed geometry of the tissue PHV, and (D) the optimized xSIBS-PHV.

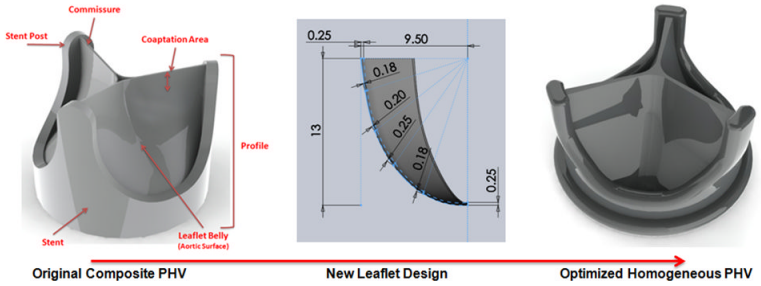

Figure 2.
Design optimization starting with the original composite polymer PHV geometry (left), the new leaflet's radial profile (center), and the new optimized PHV design (right).

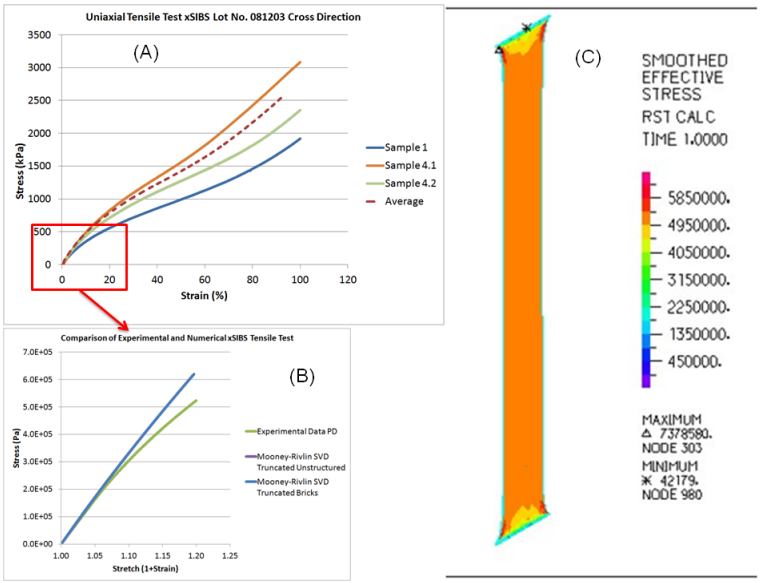

Figure 3.
(A) Uniaxial xSIBS tensile test results, (B) FEA replication and comparison to the tensile test data, (C) Stress distribution in the xSIBS sample of the simulated tensile testing.

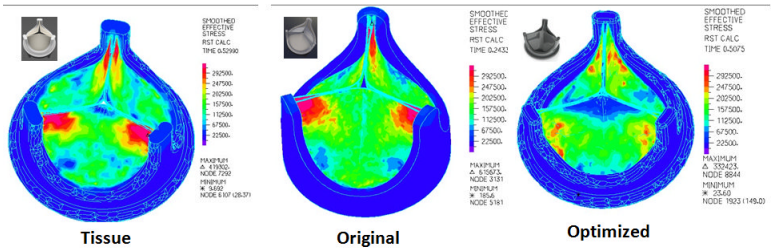

Figure 4.
Normal diastolic pressure loading results showing reduced stress concentrations in the optimized PHV (right) compared to the original composite polymer (center) and the tissue (left) PHVs.

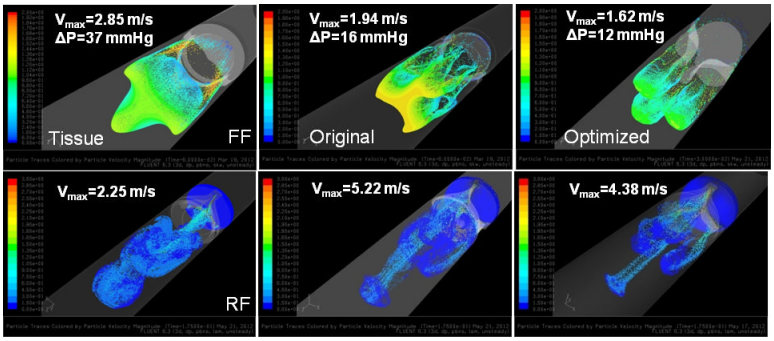

Figure 5.
Platelet dispersion patterns in the three valves during the forward (FF- top) and regurgitant (RF- bottom) flow phases from CFD.

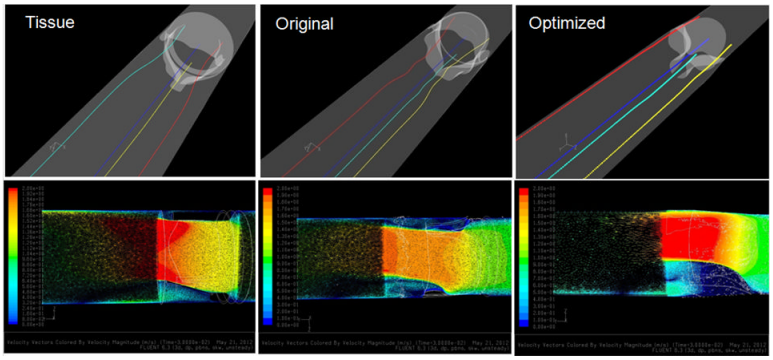

Figure 6.
Forward flow phase images of the selected platelet trajectories emulated in the HSD (top) and axial cross-sectional velocity vectors (bottom).

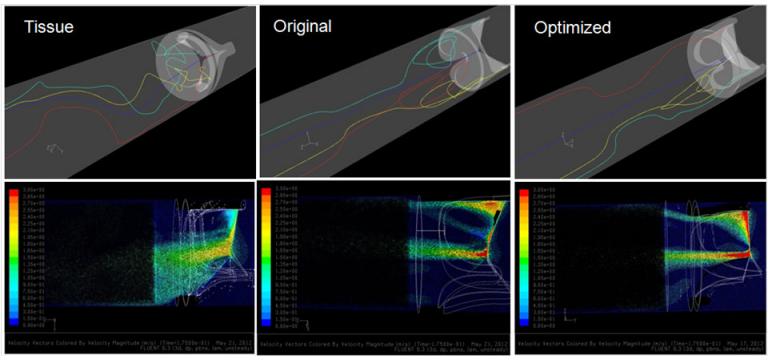

Figure 7.
Regurgitant flow phase images of the selected platelet trajectories emulated in the HSD (top) and axial cross-sectional velocity vectors (bottom).

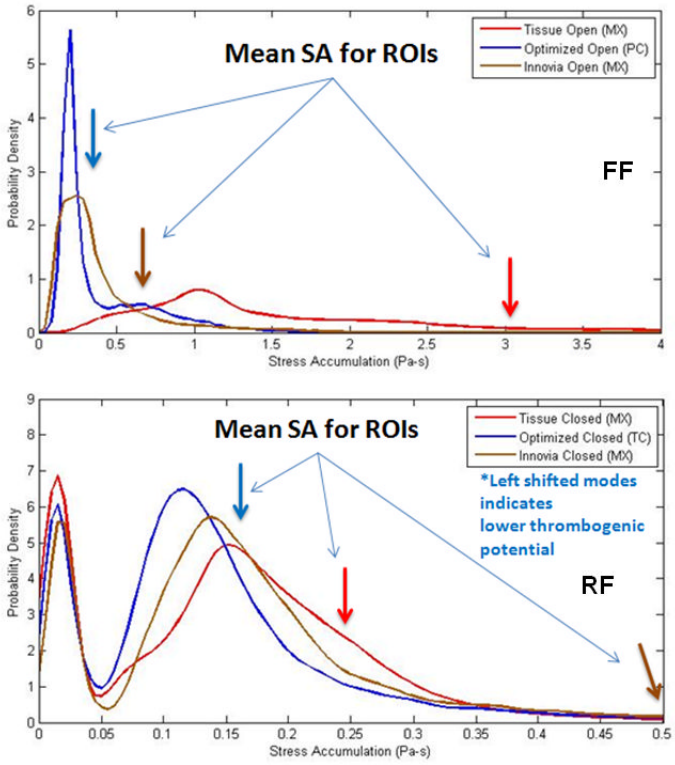

Figure 8.
Thrombogenic Footprints showing the SA distributions of each valve for forward (FF- top) and regurgitant (RF- bottom) flow phases. Both predict the lowest thrombogenicity in the optimized PHV.

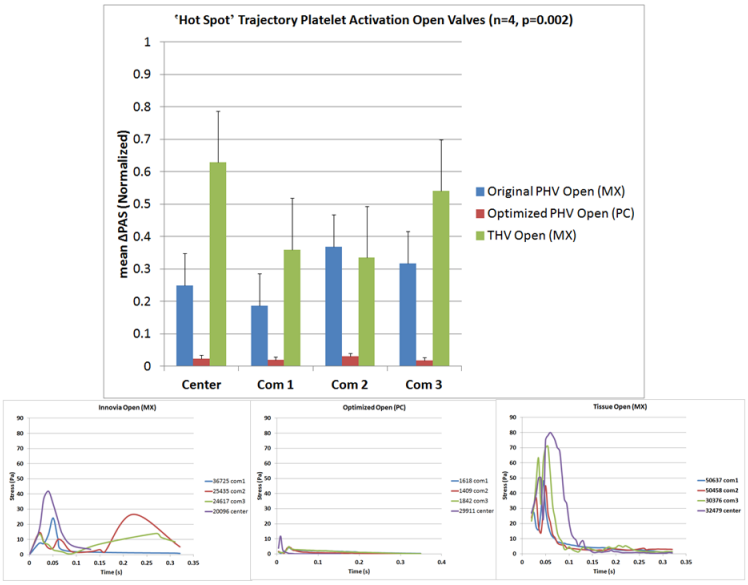

Figure 9.
Forward flow platelet activation measurement results (top) and stress-time waveforms programmed into the HSD for each valve (bottom).

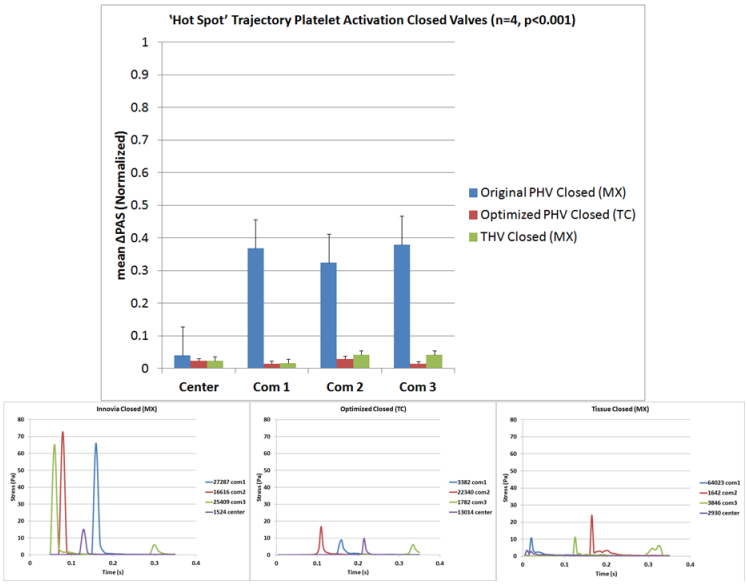

Figure 10.
Regurgitant flow platelet activation measurement results (top) and stress-time waveforms programmed into the HSD for each valve (bottom).

Table 1

FF=forward flow; RF= regurgitant flow; ΔP= pressure gradient; u=velocity; SA= stress accumulation; EOA= calculated effective orifice area 31.

	ΔP FF (mmHg)	**u_{max} FF (m/s)**	**u_{max} RF (m/s)**	**SA_{mean} FF (dyne·s/cm^2)**	**SA_{mean} RF (dyne·s/cm^2)**	**EOA FF (cm^2)**
Original	16	1.94	5.22	8.02	2.50	1.25
Tissue	37	2.85	2.25	16.35	1.95	0.83
Optimized	12	1.62	4.38	4.08	1.78	1.44

Table 2

Comparison of mean SA and mean ΔPAS values in both forward and regurgitant flow of the selected platelet trajectories.

	Open Valves		Closed Valves	
	Mean SA (dyne·s/cm^2)	**Mean ΔPAS**	**Mean SA (dyne·s/cm^2)**	**Mean ΔPAS**
Tissue	33.6	47%	2.5	3%
Original	7.3	28%	6.9	28%
Optimized	3.4	2%	1.6	2%